SNHG12 promotes chondrocyte autophagy by blocking he mTOR-primary cilia-mTOR loop via activating the miR-181a-5p/miR-138-5p-INPP5E axis

Jing Ding
Shanghai Jiao Tong University
Lin Sha
Shanghai Jiao Tong University
Lei Liu
The Affiliated Yixing Hospital of Jiangsu University
Zhenkai Wu (wuzhenkai@xinhuamed.com.cn)
Shanghai Jiao Tong University
Weijia Feng
Shanghai Jiao Tong University

Research Article

Keywords: Chondrocytes, SNHG12, hsa-miR-181a-5p, hsa-miR-138-5p, INPP5E, primary cilia, autophagy

Posted Date: May 9th, 2022

DOI: https://doi.org/10.21203/rs.3.rs-1622727/v1

Abstract

Chondrocytes are the only cell type found in normal cartilage. In this study, RT-PCR results showed that silencing INPP5E inhibited the mRNA expressions of IFT88, Beclin1, MAP1LC3A, MAP1LC3B, PI3K, Akt, mTOR, COL2A1 and CCND1 in chondrocytes. WB results showed that silencing INPP5E inhibited the protein expressions of IFT88, Beclin1, LC3 I, LC3 II, phosphorylated(p)-PI3K, p-Akt, p-mTOR, collagen II and cyclin D1 in chondrocytes. Immunofluorescence results showed that silencing INPP5E inhibited acetylated α-tubulin and LC3 II in chondrocytes. RT-PCR, WB and dual luciferase assay showed that SNHG12 promoted the expression of INPP5E by inhibiting hsa-miR-181a-5p or hsa-miR-138-5p. Functional recovery experiments show that SNHG12 regulated the expression of IFT88, Beclin1, LC3 I, LC3 II, p-PI3K, p-Akt, p-mTOR, collagen II and cyclin D1 via hsa-miR-181a-5p/hsa-miR-138-5p-INPP5E axis in chondrocytes. Our results provide a theoretical basis for the treatment of patients with cartilage abnormalities related diseases.

1. Introduction

It is reported that there are many diseases related to cartilage abnormalities, such as arthropathies, relapsing polychondritis and chondrocalcinosis, which seriously harm human health[1]. Chondrocytes are the only cell type in normal cartilage. Understanding the pathology and function of chondrocytes is very important in cartilage repair and cartilage engineering[2].

Primary cilia are multifunctional sensory organelles that regulate various signal transduction and cellular activities, and play crucial roles in the regulation of chondrogenesis[3]. Inositol polyphosphate-5-phosphatase E (INPP5E) is a transporter protein localized on the primary cilia membrane, and regulates the development and homeostasis of primary cilia[4]. INPP5E is reported to maintain stability of primary cilia[5]. INPP5E mutation or absence leads to primary ciliary signal transduction deficiency[4].

Primary cilia, as mechanical sensors, play a key role in limiting rapamycin complex 1 (mTORC1) signal transduction by converting mechanical signals into chemical activity[6]. Therefore, INPP5E may participate in mTORC1 signal transduction by regulating primary cilia. Recently, a potential link between primary cilia and autophagy has been proposed that may increase our understanding of the pathogenesis of cartilage associated diseases[7]. Autophagy, as an intracellular degradation system, maintains the homeostasis of intracellular energy metabolism and has been shown to modulate the function of damaged chondrocytes[8]. Moreover, it is reported that each step of autophagy is regulated by the target protein mTORC1[9]. Therefore, INPP5E may participate in regulating autophagy via primary cilia- mTORC1 signal transduction.

The competitive endogenous RNA (ceRNA) hypothesis proposes that transcripts with shared microRNA (miRNA) binding sites compete for post-transcriptional control[10]. However, the mechanism of ceRNA involving INPP5E is rarely reported. Our study sheds light on the following important connections

between ceRNA, INPP5E, primary cilia, autophagy, mTORC1 and chondrocytes. We aim to provide new insights into the physiological mechanisms involved in chondrocytes.

2. Materials And Methods

2.1. Bioinformatics information

The next generation sequencing of 23 cartilage knee was performed via the [HuGene-1_1-st] Affymetrix Human Gene 1.1 ST Array [transcript (gene) version] platform[11]. R language software package “limma” was used to screen differentially expressed genes (DEGs) in INPP5E-low expression (N = 11) and INPP5E-high expression (N = 12) group. $P < 0.05$ and fold change > = 2 was regarded as significance. We use the Kyoto Encyclopedia of Genes and Genomes (KEGG) database (https://www.kegg.jp/kegg/rest/keggapi.html) to obtain the latest KEGG Pathway gene annotation, as the background, to map genes to background in the collection. R software package clusterProfiler (Version 3.14.3) was used for enrichment analysis to obtain the results of gene set enrichment. $P < 0.05$ was considered as significant difference. For Gene set Enrichment analysis (GSEA), we obtained the GSEA software (version 3.0) from GSEA Database (http://software.broadinstitute.org/gsea/index.jsp), and download the c2.cp.kegg.v7.4.symbols.gmt from the Molecular Signatures Database (http://www.gsea-msigdb.org/gsea/downloads.jsp) to evaluate the pathways and molecular mechanisms. $P < 0.05$ was considered as significant difference.

2.2. Cell culture

The C28/I2 cell line (normal human chondrocytes) was provided by Zhongqiao Xinzhou Biotechnology Co., LTD (Shanghai, China). The cells were cultured in RPMI-1640 medium (Zhongqiao Xinzhou Biotechnology Co., LTD, Shanghai, China) containing 10% FBS (Zhongqiao Xinzhou Biotechnology Co., LTD, Shanghai, China) and 100 U/mL penicillin (Zhongqiao Xinzhou Biotechnology Co., LTD, Shanghai, China) and streptomycin (Zhongqiao Xinzhou Biotechnology Co., LTD, Shanghai, China). All cells were cultured in a humidified incubator containing 5% CO2 at 37°C.

2.3. Cell transfection and treatment

A total of $1*10^6$ C28/I2 cells were inoculated in 6-well plates, and lip3000 was used to transfect the corresponding plasmid or small interfering RNA (siRNA) (Supplement table 1). Follow-up experiments were performed 72 hours after transfection. All reagents were provided by Guangdong Ruibo Biotechnology Co., LTD., China.

2.4. Chloral hydrate (CH) and rapamycin (rapa) treatment

CH has a well-characterized function in chemically removing primary cilia[12]. For CH group, C28/I2 cells ($2*10^5$ cells/well) were cultured in RPMI-1640 medium with CH (Sigma-Aldrich, Merck, USA) at concentrations of 8 mM for 48h to remove primary cilia from C28/I2 cells. Rapamycin (HY-10219, MedChemExpress, China) is an effective and specific inhibitor of mTOR. For rapa group, C28/I2 cells (2

*10^5 cells/well) were cultured in RPMI-1640 medium with 0.1 nM rapa for 48h. For CH + rapa group, C28/I2 cells (2 *10^5 cells/well) were cultured in RPMI-1640 medium with 8 mM CH and 0.1 nM rapa for 48h.

2.5. Real-time fluorescence quantitative PCR (RT–PCR)

Trizol was used to extract total RNA from cells. Total RNA was reverse into cDNA via using RT Master Mix for qPCR (gDNA digester plus, MedChemExpress, China). POWER SYBR GREEN PCR MASTER (4368708, Applied Biosystems, USA) was used for PCR detection. All primers used in this study are shown in supplement table 2. The relative expression was calculated with $2^{-\triangle\triangle Ct}$ value.

2.6. Western blotting (WB)

The proteins in C28/I2 cells were extracted by RIPA and quantified using BCA kit (C503021, Sangong Bioengineering Co., LTD., Shanghai, China). Proteins were added to SDS–PAGE and transferred to polyvinylidene difluoride membranes (Millipore, USA). The transferred membranes were blocked with TBS-T (0.1% Tween-20 and TBS) containing 5% skim milk for 30 min and were then incubated overnight at 4°C with primary antibodies (Supplement table 3). Membranes were washed three times for 10 min with TBS-T and incubated for 1 h at room temperature (RT) with HRP-conjugated secondary antibodies (Supplement table 3). The protein bands were visualized by enhanced chemiluminescence using a ECL kit (AB133406, abacam, USA). Images were obtained using Sigmatel software V2.0, and protein density was calculated using Image Lab software V3.0.

2.7. Immunofluorescence

Cells were fixed with 4% paraformaldehyde in PBS for 15 min at RT and then were permeabilized with 50 lg/mL digitonin in PBS containing 0.1% gelatin for 5 min at RT, and blocked with PBS containing 0.1% gelatin for 30 min at RT. Cells were incubated with primary antibodies in PBS containing 0.1% gelatin for 60 min. After three washes with PBS, cells were incubated with the appropriate secondary antibodies in PBS contain- ing 0.1% gelatin for 50 min. Coverslips were mounted onto slides using PermaFluor mountant medium (Thermo Fisher Scientific, USA) and observed under a FluoView 1000-D confocal microscope equipped with 63x/NA 1.40 oil immersion objective lens (Olympus, Japan), or a Delta Vision microscopic system equipped with 60x/NA 1.42 oil immersion objective lens (Applied Precision). Delta Vision SoftWoRx software was used to deconvolve the images. Immunofluorescent double-staining was performed using Anti-LC3B antibody [EPR18709] - Autophagosome Marker (ab192890, Abacam, USA), Anti-alpha Tubulin (acetyl K40) [EPR16772] (ab218591, Abacam, USA) and Alexa Fluor 594 labeled goat anti-rabbit IgG (H + L; 33112ES60, Yeasen-Shanghai).

2.8. Luciferase report

The miRNA targets of INPP5E were predicted via Targetscan database (https://www.targetscan.org/vert_80/). The long non-coding RNA (lncRNA) targets of hsa-miR-181a-5p and hsa-miR-138-5p were predicted via starbase database (https://starbase.sysu.edu.cn/). A total of 1*10^5 C28/I2 cells were inoculated into 96-well plates for 24h and transfected into luciferase reporter

plasmid: Firefly (Luciferase Reporter Assay Substrate Kit - Firefly, AB228530, ABACAM, USA) and Renilla (Luciferase Reporter Assay Substrate Kit-Renilla, AB228546, USA). Based on the binding sites predicted by targetscan database and Starbase Database, the pMIR-INPP5E-mutant (mut) 3' UTR plasmid, pMIR-SNHG12-mut-1 3' UTR plasmid (according to the binding site of SNHG12 and hsa-miR-181a-5p) and pMIR-SNHG12-mut-2 3' UTR plasmid (according to the binding site of SNHG12 and hsa-miR-138-5p) were constructed. pMIR- INPP5E-wild type (WT) 3 'UTR plasmid and all mutated plasmids were provided by heyuan biology co., LTD. (Shanghai, China). Each plasmid was co-transfected with luciferase reporter plasmid for 48h, and 100μl Stop&Glo Reagent was added per well. Fluorescence was detected at wavelength 480nm (SpectraMax M2e Molecular Devices, USA).

2.9. Statistical analysis

SPSS 21.0 (International Business Machines Corporation, NY, USA) was used for data collection, expressed as Mean ± SD. All Experiments were performed independently at least three times, the comparison method of the two groups was Wilcox tests. $P < 0.05$ was considered statistically significant.

3. Results

3.1. INPP5E de-activated the PI3K-Akt-mTOR signaling pathway in vitro

Based on GSE43191 data set, we divided the samples into INPP5E-low expression (N = 11) group and INPP5E-high expression (N = 12) group. Using $P < 0.05$ and fold change > = 2 as screening criteria, we found that 998 genes were differentially expressed in the INPP5e-high expression (N = 12) group compared with the INPP5e-low expression (N = 11) group (Fig. 1A). KEGG analysis (Fig. 1B) and GSEA analysis (Fig. 1C) showed that these genes were significantly enriched in PI3K-Akt and mTOR signaling pathway. Together, INPP5E might be involved in the regulation of PI3K-Akt and mTOR signaling pathway. Compared with control or NC group, the mRNA expression of INPP5E was significant reduced in si-INPP5E-2 and si-INPP5E-3 group via RT-PCR detection (Fig. 1D). Compared with WT or NC group, the protein expression of INPP5E was significant reduced in si-INPP5E-2 group via WB detection (Fig. 1E). Silencing INPP5E up-regulated the mRNA expression of PI3K, Akt and mTOR in chondrocytes via RT-PCR detection (Fig. 1F). Although there was no significant difference of the protein expression of PI3K, Akt and mTOR between control, NC and si-INPP5E-2 group, while silencing INPP5E up-regulated the protein expression of p-PI3K, p-Akt and p-mTOR in chondrocytes via WB detection (Fig. 1G). Together, silencing INPP5E activated the PI3K-Akt-mTOR signaling pathway in vitro.

3.2. INPP5E promotes autophagy via regulating the mTOR-primary cilia- mTOR loop

Silencing INPP5E inhibited the mRNA expression of IFT88, Beclin1, MAP1LC3A and MAP1LC3B (Fig. 2A), and inhibited the protein expression of IFT88, Beclin1, LC3 I and LC3 II (Fig. 2B). These results suggest

that silencing INPP5E inhibits primary cilia and autophagy. Compared with control group, the mRNA expression of IFT88, Beclin1, MAP1LC3A, MAP1LC3B, PI3K, Akt and mTOR were down-regulated expression in CH-treated group (Fig. 2C). Although, there was no significant difference of the protein expression of PI3K, Akt and mTOR between control and CH-treated group, while compared with control group, the protein expression of IFT88, Beclin1, LC3 I, LC3 II, p-PI3K, p-Akt and p-mTOR were down-regulated expression in CH-treated group (Fig. 2D). These results suggest that inhibition of primary cilia reduces autophagy and inhibits the activation of PI3K-Akt-mTOR signaling pathway in chondrocytes. Compared with control group, silencing INPP5E inhibited the protein expression of ace-tubulin and LC3 I/II, while silencing mTOR (rapamycin-treated group) promoted the protein expression of ace-tubulin and LC3 I/II (Fig. 2E). Compared with rapamycin-treated group, the protein expression of ace-tubulin and LC3 I/II was reduced in si-INPP5E + rapamycin-treated group (Fig. 2E). These results suggest that silencing INPP5E inhibits primary cilia and autophagy by activating mTOR. Compared with control group, the protein expression of ace-tubulin and LC3 I/II was reduced in CH-treated group. Compared with CH-treated group, the protein expression of ace-tubulin and LC3 I/II was enhanced in rapamycin-treated + CH-treated group (Fig. 2E). These results suggest that INPP5E silencing inhibits primary cilia and autophagy by activating mTOR. These results suggest that silencing INPP5E inhibits autophagy via inhibiting primary cilia-induced mTOR inactivation. Together, silencing INPP5E inhibits autophagy via promoting primary cilia-induced PI3K-Akt-mTOR signaling pathway activation, and the activated PI3K-Akt-mTOR signaling pathway further reducing autophagy via inhibiting primary cilia.

3.3. The SNHG12-hsa-miR-181a-5p/hsa-miR-138-5p-INPP5E ceRNA network in vitro

Targetscan database was used to predict miRNAs that might bind to INPP5E (Supplement Fig. 1). It was reported that over-expression of hsa-miR-4262 promoted autophagy in chondrocyte[13]. However, over-expression of hsa-miR-181a-5p inhibited hunger-induced cardiac autophagy[14], and over-expression of hsa-miR-138-5p inhibited MnCl2-induced autophagy in SH-SY5Y cells[15]. Therefore, we speculated that high expression of hsa-miR-181a-5p and hsa-miR-138-5p might inhibit autophagy of chondrocytes by inhibiting INPP5E. Compared with control or NC group, the expression of hsa-miR-181a-5p was increased significant in mimic-1 group (Fig. 3A). Over-expression of hsa-miR-181a-5p inhibited the mRNA (Fig. 3B) and protein (Fig. 3C) expression of INPP5E in chondrocytes. Compared with mimic-NC group, the relative intensity of fluorescence in mimic-1 group was reduced significant in INPP5E-WT chondrocytes. However, there was no significant difference of the relative intensity of fluorescence between mimic-NC and mimic-1 group in INPP5E-Mut chondrocytes via dual luciferase reported assay (Fig. 3D). Compared with control or NC group, the expression of hsa-miR-138-5p was increased significant in mimic-2 group (Fig. 3E). Over-expression of hsa-miR-138-5p inhibited the mRNA (Fig. 3F) and protein (Fig. 3G) expression of INPP5E in chondrocytes. Compared with mimic-NC group, the relative intensity of fluorescence in mimic-2 group was reduced significant in INPP5E-WT chondrocytes. However, there was no significant difference of the relative intensity of fluorescence between mimic-NC and mimic-2 group in INPP5E-Mut chondrocytes via dual luciferase reported assay (Fig. 3H). Based on Starbase database, we found that 5 lncRNAs may be

common targets of hsa-miR-181a-5p and hsa-miR-138-5p (Fig. 3I). Over-expression of SNHG12 is reported to promote autophagy of the SH-SY5Y cells [16]. Therefore, SNHG12 may promote chondrocyte autophagy through up-regulation of INPP5E.Compared with control or NC group, the expression of SNHG12 was reduced significant in si-SNHG12-2 and si-SNHG12-3 group (Fig. 3J). Silencing SNHG12 promoted the expression of hsa-miR-181a-5p and hsa-miR-138-5p in chondrocytes (Fig. 3K). Compared with mimic-NC group, the relative intensity of fluorescence in mimic-1 group was reduced significant in SNHG12-WT chondrocytes. However, there was no significant difference of the relative intensity of fluorescence between mimic-NC and mimic-1 group in SNHG12-Mut-1 chondrocytes via dual luciferase reported assay (Fig. 3L). Compared with mimic-NC group, the relative intensity of fluorescence in mimic-2 group was reduced significant in SNHG12-WT chondrocytes. However, there was no significant difference of the relative intensity of fluorescence between mimic-NC and mimic-2 group in SNHG12-Mut-2 chondrocytes via dual luciferase reported assay (Fig. 3M). Together, SNHG12 promoted the expression of INPP5E via decreasing hsa-miR-181a-5p and hsa-miR-138-5p expression in chondrocytes.

3.4. SNHG12 inhibits primary cilia and autophagy via hsa-miR-181a-5p/hsa-miR-138-5p-INPP5E axis in chondrocytes

Compared with control or NC group, the mRNA (Fig. 4A) and protein (Fig. 4B) expression of INPP5E was enhanced significant in OE-INPP5E group. Compared with control or NC group, the mRNA (Fig. 4C) and protein (Fig. 4D) expression of INPP5E was reduced significant in si-INPP5E group. Compared with control or NC group, the mRNA (Fig. 4E) and protein (Fig. 4F) expression of IFT88, beclin1, LC3 I and LC3 II was reduced significant in mimic-1 group. Compared with mimic-1 group, the mRNA (Fig. 4E) and protein (Fig. 4F) expression of IFT88, beclin1and LC3 I was enhanced significant in mimic-1 + OE-INPP5E group. Compared with control or NC group, the mRNA (Fig. 4G) and protein (Fig. 4H) expression of IFT88, beclin1, LC3 I and LC3 II was reduced significant in mimic-2 group. Compared with mimic-2 group, the mRNA (Fig. 4G) and protein (Fig. 4H) expression of IFT88, beclin1and LC3 I was enhanced significant in mimic-2 + OE-INPP5E group. Compared with control or NC group, the mRNA (Fig. 4I) and protein (Fig. 4J) expression of IFT88, beclin1, LC3 I and LC3 II was reduced significant in si-SNHG12 group. Compared with si-SNHG12 group, the mRNA (Fig. 4I) and protein (Fig. 4J) expression of IFT88, beclin1and LC3 I was enhanced significant in si-SNHG12 + OE-INPP5E group. Compared with control or NC group, the protein expression of ace-tubulin and LC3 I/II was increased significant in OE-INPP5E group. Compared with OE-INPP5E group, the protein expression of ace-tubulin and LC3 I/II was decreased significant in si-SNHG12 + OE-INPP5E group, mimic-1 + OE-INPP5E group or mimic-2 + OE-INPP5E group (Fig. 4K). Together, silencing SNHG12 promoted primary cilia and autophagy via hsa-miR-181a-5p/hsa-miR-138-5p-INPP5E axis in chondrocytes.

3.5. SNHG12 de-activates the PI3K-Akt-mTOR signaling pathway via hsa-miR-181a-5p/hsa-miR-138-5p-INPP5E axis in vitro

Compared with control or NC group, the mRNA expression of PI3K, Akt and mTOR was enhanced in mimic-1 group. Compared with mimic-1 group, the mRNA expression of PI3K, Akt and mTOR was reduced in mimic-1 + OE-INPP5E group (Fig. 5A). Compared with control or NC group, the protein expression of p-PI3K, p-Akt and p-mTOR was enhanced in mimic-1 group. Compared with mimic-1 group, the protein expression of p-PI3K, p-Akt and p-mTOR was reduced in mimic-1 + OE-INPP5E group (Fig. 5B). However, there was no significance of the protein expression of PI3K, Akt and mTOR among control, NC, mimic-1 and mimic-1 + OE-INPP5E group in chondrocytes (Fig. 5B). Compared with control or NC group, the mRNA expression of PI3K, Akt and mTOR was enhanced in mimic-2 group. Compared with mimic-1 group, the mRNA expression of PI3K, Akt and mTOR was reduced in mimic-2 + OE-INPP5E group (Fig. 5C). Compared with control or NC group, the protein expression of p-PI3K, p-Akt and p-mTOR was enhanced in mimic-1 group. Compared with mimic-2 group, the protein expression of p-PI3K, p-Akt and p-mTOR was reduced in mimic-2 + OE-INPP5E group (Fig. 6D). However, there was no significance of the protein expression of PI3K, Akt and mTOR among control, NC, mimic-2 and mimic-2 + OE-INPP5E group in chondrocytes (Fig. 5D). Compared with control or NC group, the mRNA expression of PI3K, Akt and mTOR was enhanced in si-SNHG12 group. Compared with si-SNHG12 group, the mRNA expression of PI3K, Akt and mTOR was reduced in si-SNHG12 + OE-INPP5E group (Fig. 5E). Compared with control or NC group, the protein expression of p-PI3K, p-Akt and p-mTOR was enhanced in si-SNHG12 group. Compared with si-SNHG12 group, the protein expression of p-PI3K, p-Akt and p-mTOR was reduced in si-SNHG12 + OE-INPP5E group (Fig. 6F). However, there was no significance of the protein expression of PI3K, Akt and mTOR among control, NC, si-SNHG12 and si-SNHG12 + OE-INPP5E group in chondrocytes (Fig. 5F). Together, silencing SNHG12 activated the PI3K-Akt-mTOR signaling pathway via hsa-miR-181a-5p/hsa-miR-138-5p-INPP5E axis in chondrocytes.

3.6. SNHG12 promotes the expression of collagen II and cyclin D1 via hsa-miR-181a-5p/hsa-miR-138-5p-INPP5E axis in vitro

Compared with control or NC group, the mRNA expression of COL2A1 and CCND1 was reduced and the protein expression of collagen II and cyclin D1 was reduced in si-INPP5E group (Fig. 6A and B). Compared with control or NC group, the mRNA expression of COL2A1 and CCND1 was reduced and the protein expression of collagen II and cyclin D1 was reduced in mimic-1 group (Fig. 6C and D) or in mimic-2 group (Fig. 6E and F). Compared with mimic-1 group or mimic-2 group, the mRNA expression of COL2A1 and CCND1 was increased and the protein expression of collagen II and cyclin D1 was increased in mimic-1 + OE-INPP5E group (Fig. 6C and D) or in mimic-2 + OE-INPP5E group (Fig. 6E and F), respectively. Compared with control or NC group, the mRNA expression of COL2A1 and CCND1 was reduced and the protein expression of collagen II and cyclin D1 was reduced in si-SNHG12 group (Fig. 6G and H). Compared with si-SNHG12 group, the mRNA expression of COL2A1 and CCND1 was increased and the protein expression of collagen II and cyclin D1 was increased in si-SNHG12 + OE-INPP5E group (Fig. 6C and D). Together, silencing SNHG12 inhibits the expression of collagen II and cyclin D1 via hsa-miR-181a-5p/hsa-miR-138-5p-INPP5E axis in chondrocytes.

4. Discussion

Primary cilia are hornlike sensory organelles that play an important role in regulating the function of chondrocyte[17]. INPP5E regulates mitosis and ciliary disassembly of primary cilia[5]. However, the regulation of INPP5E on primary cilia in chondrocytes has not been reported. IFT88 is a core component of the intracflagellar transport complex B and is essential for cilia construction[18]. Downregulation or loss of IFT88 is known to impair cilia occurrence[19]. Ace-tubulin is a key protein in regulating ciliary peristalsis and controlling its stability[20]. In this study, we found that silencing INPP5E inhibited the expression of IFT88 and ace-tubulin, suggesting that inhibition of INPP5E reduced primary cilia formation in chondrocytes.

Recent studies have shown that activation of autophagy requires primary cilia, and that autophagy is involved in controlling cilia formation[21]. In this study, we treated chondrocytes with CH, the expression of beclin-1, LC3 I and LC3 II were reduced significantly. The elevated expression of beclin-1, LC3 I or LC3 II was positive associated with the level autophagy[22, 23]. These results further suggest that inhibition of primary cilia reduces chondrocytes autophagy.

MiRNAs are small non-coding RNAs that inhibit gene mRNA expression by interfering with transcription[24]. In this study, two miRNAs hsa-miR-181a-5p and hsa-miR-138-5p were found bound with INPP5E, and inhibits its expression. Hsa-miR-181a-5p inhibits autophagy in MCF-10A cells[25]. Hsa-miR-138-5p inhibits autophagy in pancreatic cancer cells[26]. Over-expression of hsa-miR-181a-5p or hsa-miR-138-5p inhibits beclin-1, LC3 I or LC3 II in chondrocytes. Over-expression of hsa-miR-181a-5p or hsa-miR-138-5p inhibits the promoting effect of INPP5E on beclin-1, LC3 I or LC3 II in chondrocytes. Therefore, hsa-miR-181a-5p or hsa-miR-138-5p inhibits autophagy of chondrocytes by inhibiting INPP5E.

The effect of hsa-miR-181a-5p or hsa-miR-138-5p on primary cilia has not been reported. In the current study, over-expression of hsa-miR-181a-5p or hsa-miR-138-5p inhibits IFT88 and ace-tubulin in chondrocytes, suggesting that hsa-miR-181a-5p or hsa-miR-138-5p inhibits autophagy of chondrocytes by inhibiting primary cilia. Moreover, over-expression of hsa-miR-181a-5p or hsa-miR-138-5p inhibits the promoting effect of INPP5E on IFT88 and ace-tubulin in chondrocytes. Therefore, hsa-miR-181a-5p or hsa-miR-138-5p down-regulates chondrocyte autophagy by inhibiting inPP5E-induced primary cilia.

CeRNAs are mutually regulated transcripts of competing shared miRNAs at the post-transcriptional level. The CeRNA network links the function of mRNAs to non-coding RNAs such as miRNAs, lncRNAs, and circRNAs[27]. In this study, SNHG12 was found bound with hsa-miR-181a-5p or hsa-miR-138-5p, and inhibits its expression. SNHG12 has been reported to promote autophagy[16]. In this study, the role of SNHG12 in promoting autophagy was also confirmed in chondrocytes. Moreover, silencing SNHG12 inhibits the promoting effect of INPP5E on beclin-1, LC3 I or LC3 II in chondrocytes. Therefore, SNHG12 promotes autophagy of chondrocytes through the hsa-miR-181a-5p/hsa-miR-138-5p-INPP5E axis. In addition, we found for the first time that SNHG12 promotes the expression of IFT88 and ace-tubulin in chondrocytes. Silencing SNHG12 inhibits the promoting effect of INPP5E on IFT88 and ace-tubulin in

chondrocytes. Therefore, SNHG12 promotes chondrocyte autophagy by promoting INPP5E-induced primary cilia formation.

Inhibition of mTORC1 signaling by primary cilia has been demonstrated[6]. In this study, we also found that after treating chondrocytes with CH, the protein expression of p-mTOR was increased. Interestingly, expression of ace-tubulin was elevated when we treated chondrocytes with rapa. Therefore, there exists a mTOR-primary cilia-mTOR loop in chondrocytes. MTOR is a highly conserved kinase that is important for autophagy regulation[28].In this study, we found that inhibition of mTOR promotes the autophagy in chondrocytes. In addition, inhibition of INPP5E reduced the promoting effect of rapa on autophagy. Therefore, INPP5E promotes chondrocyte autophagy by inhibiting mTOR-primary cilia-mTOR loop.

Collagen II is one of the cross-linked copolymers of the core fiber network during chondrogenesis[29]. Articular cartilage maintains its function based on the longevity of Collagen II [30]. Silencing INPP5E inhibits the expression of collagen II in chondrocytes. Silencing SNHG12 or over-expression of hsa-miR-181a-5p or hsa-miR-138-5p inhibits the promoting effect of INPP5E on collagen II in chondrocytes. These results suggest that SNHG12 promotes collagen II through hsa-miR-181a-5p/hsa-miR-138-5p- INPP5E axis in chondrocytes. The proliferation and maturation of chondrocytes requires attachment to a matrix rich in collagen II[31]. Thus, SNHG12 might the proliferation and maturation of chondrocytes. Dicam is reported to promote chondrocyte proliferation and maturation through hedgehog signaling pathway in primary cilia[32]. Inhibition of PI3K/AKT/mTOR signaling pathway inhibits chondrocyte proliferation[33]. Therefore, SNHG12 might promote chondrocyte proliferation and maturation by activating mTOR signal via promoting INPP5E-mediated primary cilia formation.

Cyclin D1 integrates extracellular mitotic signaling and cell cycle progression[34]. Silencing INPP5E inhibits the expression of cyclin D1 in chondrocytes. Silencing SNHG12 or over-expression of hsa-miR-181a-5p or hsa-miR-138-5p inhibits the promoting effect of INPP5E on cyclin D1 in chondrocytes. These results suggest that SNHG12 promotes collagen II through hsa-miR-181a-5p/hsa-miR-138-5p- INPP5E axis in chondrocytes. These results suggest that SNHG12 might maintain the cell cycle of chondrocytes through hsa-miR-181a-5p/hsa-miR-138-5p-INPP5E axis.

In conclusion, SNHG12 upregulates INPP5E via inhibiting hsa-miR-181a-5p/hsa-miR-138-5p in chondrocytes. INPP5E increasing autophagy of chondrocytes via de-activating the mTOR-primary cilia-mTOR loop. Our results provide a theoretical basis for the treatment of patients with cartilage abnormalities related diseases.

Declarations

Ethics approval and consent to participate

Not applicable.

Consent for publication

Not applicable.

Availability of data and materials

The datasets during and/or analyzed during the current study are available from the corresponding author on reasonable request.

Competing interests

The authors declare that they have no competing interests.

Funding

This work was supported by the Interdisciplinary Program of Shanghai Jiao Tong University (project number YG2021QN48).

Authors' contributions

All authors participated in performing the experiments and writing the paper. Zhenkai Wu and Weijia Feng supervised the study and revised the paper.

Acknowledgements

Not applicable.

References

1. Y. Krishnan, A.J. Grodzinsky, Cartilage diseases, Matrix Biol, 71–72 (2018) 51–69.
2. A.C. Hall, The Role of Chondrocyte Morphology and Volume in Controlling Phenotype-Implications for Osteoarthritis, Cartilage Repair, and Cartilage Engineering, Curr Rheumatol Rep, 21 (2019) 38.
3. F. Tao, T. Jiang, H. Tao, H. Cao, W. Xiang, Primary cilia: Versatile regulator in cartilage development, Cell proliferation, 53 (2020) e12765.
4. R. Zhang, J. Tang, T. Li, J. Zhou, W. Pan, INPP5E and Coordination of Signaling Networks in Cilia, Front Mol Biosci, 9 (2022) 885592.
5. O.V. Plotnikova, S. Seo, D.L. Cottle, S. Conduit, S. Hakim, J.M. Dyson, C.A. Mitchell, I.M. Smyth, INPP5E interacts with AURKA, linking phosphoinositide signaling to primary cilium stability, Journal of cell science, 128 (2015) 364–372.
6. Y. Lai, Y. Jiang, Reciprocal Regulation between Primary Cilia and mTORC1, Genes (Basel), 11 (2020).
7. J.Y. Ko, E.J. Lee, J.H. Park, Interplay Between Primary Cilia and Autophagy and Its Controversial Roles in Cancer, Biomol Ther (Seoul), 27 (2019) 337–341.
8. R. Duan, H. Xie, Z.Z. Liu, The Role of Autophagy in Osteoarthritis, Front Cell Dev Biol, 8 (2020) 608388.

9. T. Noda, Regulation of Autophagy through TORC1 and mTORC1, Biomolecules, 7 (2017).
10. D.W. Thomson, M.E. Dinger, Endogenous microRNA sponges: evidence and controversy, Nature reviews. Genetics, 17 (2016) 272–283.
11. J. Fernandez-Tajes, A. Soto-Hermida, M.E. Vazquez-Mosquera, E. Cortes-Pereira, A. Mosquera, M. Fernandez-Moreno, N. Oreiro, C. Fernandez-Lopez, J.L. Fernandez, I. Rego-Perez, F.J. Blanco, Genome-wide DNA methylation analysis of articular chondrocytes reveals a cluster of osteoarthritic patients, Annals of the rheumatic diseases, 73 (2014) 668–677.
12. Y.H. Li, D. Zhu, Z. Cao, Y. Liu, J. Sun, L. Tan, Primary cilia respond to intermittent low-magnitude, high-frequency vibration and mediate vibration-induced effects in osteoblasts, Am J Physiol Cell Physiol, 318 (2020) C73-C82.
13. W. Sun, Y. Li, S. Wei, miR-4262 regulates chondrocyte viability, apoptosis, autophagy by targeting SIRT1 and activating PI3K/AKT/mTOR signaling pathway in rats with osteoarthritis, Experimental and therapeutic medicine, 15 (2018) 1119–1128.
14. L. Chang, X. Chai, P. Chen, J. Cao, H. Xie, J. Zhu, miR-181b-5p suppresses starvation-induced cardiomyocyte autophagy by targeting Hspa5, International journal of molecular medicine, 43 (2019) 143–154.
15. J. Ma, Y. Zhang, H. Ji, L. Chen, T. Chen, C. Guo, S. Zhang, J. Jia, P. Niu, Overexpression of miR-138-5p suppresses MnCl2 -induced autophagy by targeting SIRT1 in SH-SY5Y cells, Environ Toxicol, 34 (2019) 539–547.
16. X. Yao, R. Yao, F. Huang, J. Yi, LncRNA SNHG12 as a potent autophagy inducer exerts neuroprotective effects against cerebral ischemia/reperfusion injury, Biochemical and biophysical research communications, 514 (2019) 490–496.
17. E.R. Moore, C.R. Jacobs, The primary cilium as a signaling nexus for growth plate function and subsequent skeletal development, J Orthop Res, 36 (2018) 533–545.
18. C. Boehlke, H. Janusch, C. Hamann, C. Powelske, M. Mergen, H. Herbst, F. Kotsis, R. Nitschke, E.W. Kuehn, A Cilia Independent Role of Ift88/Polaris during Cell Migration, PloS one, 10 (2015) e0140378.
19. J.A. Follit, F. Xu, B.T. Keady, G.J. Pazour, Characterization of mouse IFT complex B, Cell Motil Cytoskeleton, 66 (2009) 457–468.
20. D. Wloga, E. Joachimiak, P. Louka, J. Gaertig, Posttranslational Modifications of Tubulin and Cilia, Cold Spring Harb Perspect Biol, 9 (2017).
21. O. Pampliega, A.M. Cuervo, Autophagy and primary cilia: dual interplay, Curr Opin Cell Biol, 39 (2016) 1–7.
22. Y.J. Hu, J.T. Zhong, L. Gong, S.C. Zhang, S.H. Zhou, Autophagy-Related Beclin 1 and Head and Neck Cancers, OncoTargets and therapy, 13 (2020) 6213–6227.
23. B.L. Heckmann, D.R. Green, LC3-associated phagocytosis at a glance, Journal of cell science, 132 (2019).

24. L. Chen, L. Heikkinen, C. Wang, Y. Yang, H. Sun, G. Wong, Trends in the development of miRNA bioinformatics tools, Briefings in bioinformatics, 20 (2019) 1836–1852.
25. J.L. Wei, Y.C. Li, Z.L. Ma, Y.X. Jin, MiR-181a-5p promotes anoikis by suppressing autophagy during detachment induction in the mammary epithelial cell line MCF10A, Protein Cell, 7 (2016) 305–309.
26. S. Tian, X. Guo, C. Yu, C. Sun, J. Jiang, miR-138-5p suppresses autophagy in pancreatic cancer by targeting SIRT1, Oncotarget, 8 (2017) 11071–11082.
27. X. Qi, D.H. Zhang, N. Wu, J.H. Xiao, X. Wang, W. Ma, ceRNA in cancer: possible functions and clinical implications, Journal of medical genetics, 52 (2015) 710–718.
28. Y. Wang, H. Zhang, Regulation of Autophagy by mTOR Signaling Pathway, Advances in experimental medicine and biology, 1206 (2019) 67–83.
29. D. Eyre, Collagen of articular cartilage, Arthritis Res, 4 (2002) 30–35.
30. M.L. Tiku, B. Madhan, Preserving the longevity of long-lived type II collagen and its implication for cartilage therapeutics, Ageing Res Rev, 28 (2016) 62–71.
31. L. Terpstra, J. Prud'homme, A. Arabian, S. Takeda, G. Karsenty, S. Dedhar, R. St-Arnaud, Reduced chondrocyte proliferation and chondrodysplasia in mice lacking the integrin-linked kinase in chondrocytes, J Cell Biol, 162 (2003) 139–148.
32. S. Han, H.R. Park, E.J. Lee, J.A. Jang, M.S. Han, G.W. Kim, J.H. Jeong, J.Y. Choi, F. Beier, Y.K. Jung, Dicam promotes proliferation and maturation of chondrocyte through Indian hedgehog signaling in primary cilia, Osteoarthritis Cartilage, 26 (2018) 945–953.
33. F.B. Feng, H.Y. Qiu, Effects of Artesunate on chondrocyte proliferation, apoptosis and autophagy through the PI3K/AKT/mTOR signaling pathway in rat models with rheumatoid arthritis, Biomed Pharmacother, 102 (2018) 1209–1220.
34. G. Tchakarska, B. Sola, The double dealing of cyclin D1, Cell Cycle, 19 (2020) 163–178.

Figures

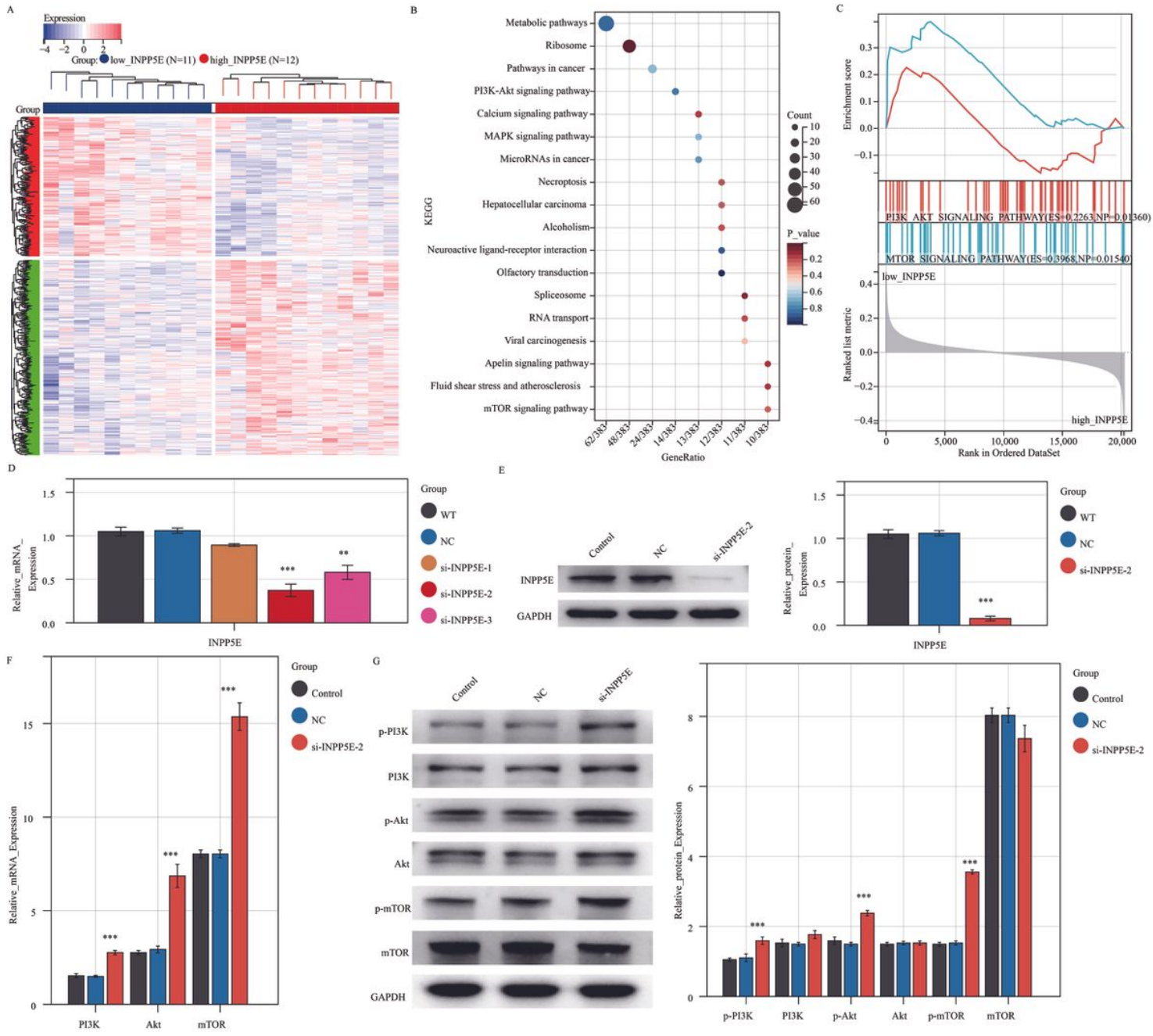

Figure 1

Silencing INPP5E activates PI3K-Akt-MTOR signaling pathway in vitro. (A) We divided the samples into INPP5E-low expression (N=11) group and INPP5E-high expression (N=12) group in GSE43191 dataset. Using P<0.05 and fold change >=2 as screening criteria, a hub of 998 DEGs were identified. (B) KEGG analysis and (C) GSEA analysis were used to analysis the pathway mechanism involved in these 998 DEGs. (D) RT-PCR assay was used to detected the expression of INPP5E. (E) WB assay was used to detected the expression of INPP5E. (F) RT-PCR assay was used to detected the expression of PI3K, Akt and mTOR. (G) WB assay was used to detected the expression of PI3K, p-PI3K, Akt, p-Akt, mTOR and p-mTOR. Notes: *p<0.05, **p<0.01, ***p<0.001 compared with control.

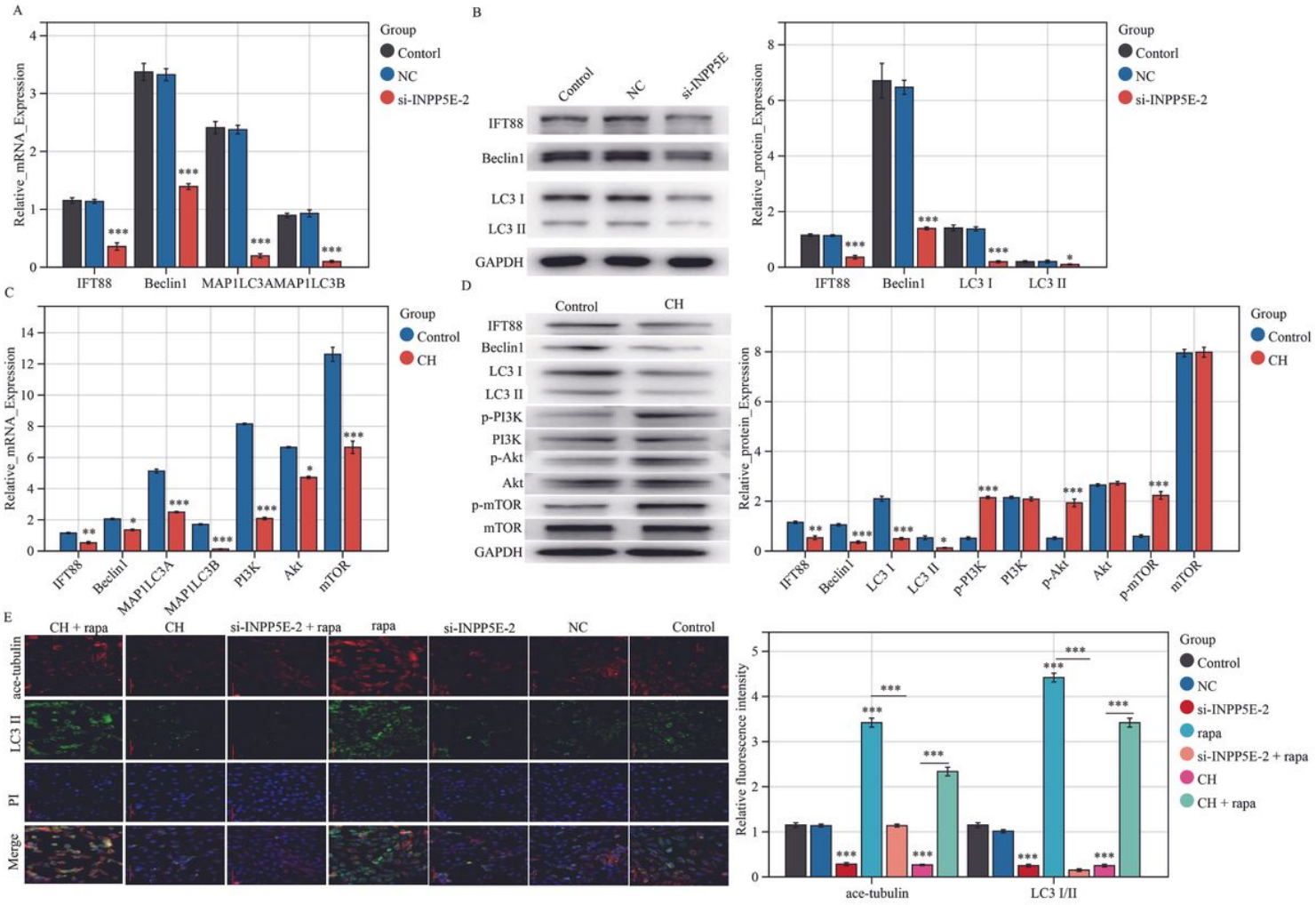

Figure 2

Silencing INPP5E inhibits autophagy via regulating the mTOR-primary cilia- mTOR loop in vitro. (A) RT-PCR assay was used to detected the mRNA expression of IFT88, Beclin1, MAP1LC3A and MAP1LC3B in control, NC and si-INPP5E-2 group. (B) WB assay was used to detected the protein expression of IFT88, Beclin1, LC3 I and LC3 II in control, NC and si-INPP5E-2 group. (C) RT-PCR assay was used to detected the mRNA expression of IFT88, Beclin1, MAP1LC3A, MAP1LC3B, PI3K, Akt and mTOR in control and CH-treated group. (D) WB assay was used to detected the protein expression of IFT88, Beclin1, LC3 I, LC3 II, p-PI3K, PI3K, p-Akt, Akt, p-mTOR and mTOR in control and CH-treated group. (E) Ace-tubulin was used to labeled primary cilia and LC3 II was used to labeled autophagy via immunofluorescence assay. Notes: *p<0.05, **p<0.01, ***p<0.001 compared with control.

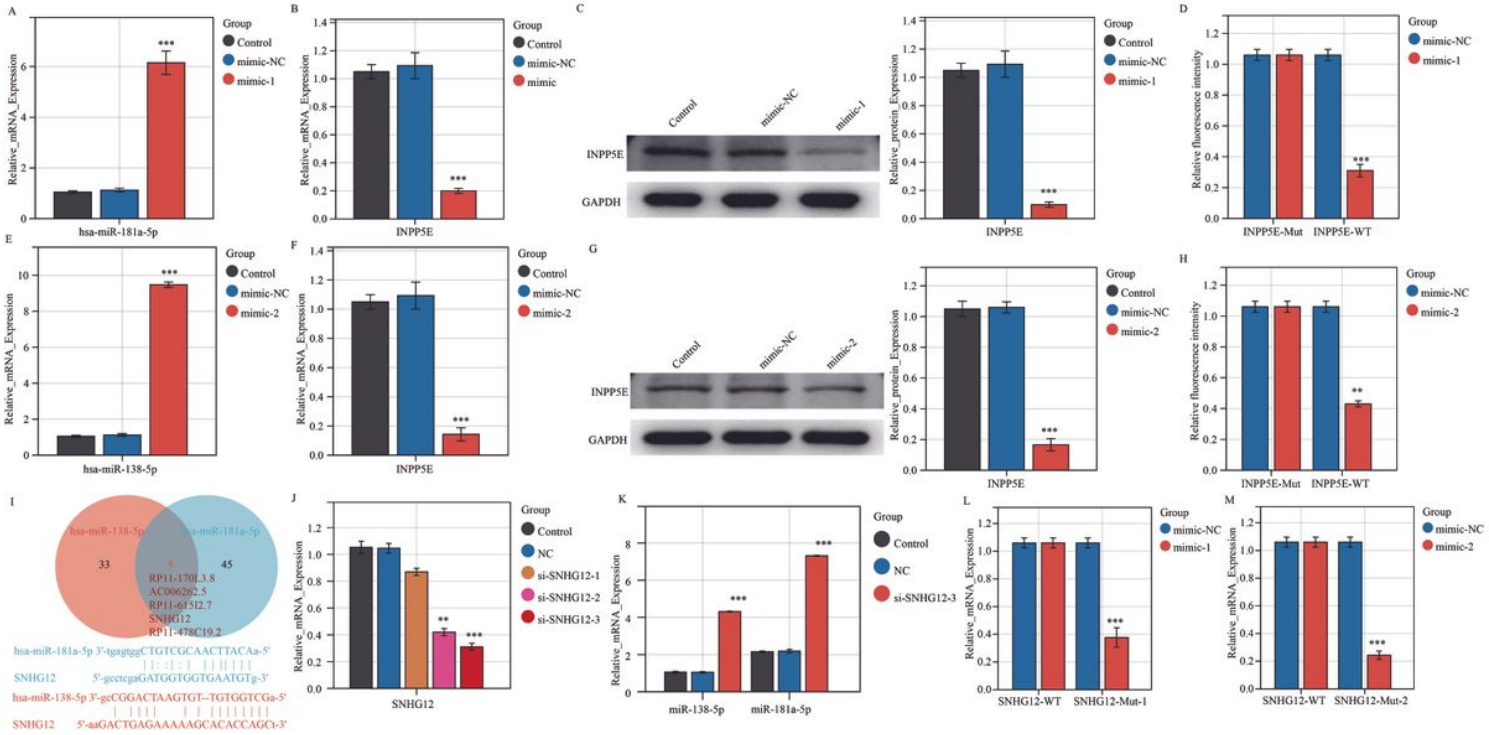

Figure 3

SNHG12 promotes the expression of INPP5E via hsa-miR-181a-5p/hsa-miR-138-5p in vitro. (A) RT-PCR assay was used to detected the expression of hsa-miR-181a-5p in control, mimic-NC and mimic-1 group. (B) RT-PCR assay was used to detected the expression of INPP5E in control, mimic-NC and mimic-1 group. (C) WB assay was used to detected the expression of INPP5E in control, mimic-NC and mimic-1 group. (D) The dual luciferase reporting assay was used to verify the binding of INPP5E to hsa-miR-181a-5p. (E) RT-PCR assay was used to detected the expression of hsa-miR-138-5p in control, mimic-NC and mimic-2 group. (F) RT-PCR assay was used to detected the expression of INPP5E in control, mimic-NC and mimic-2 group. (G) WB assay was used to detected the expression of INPP5E in control, mimic-NC and mimic-2 group. (H) The dual luciferase reporting assay was used to verify the binding of INPP5E to hsa-miR-138-5p. (I) Stabase database was used to predicted the lncRNAs that might bind to hsa-miR-181a-5p and hsa-miR-138-5p. (J) RT-PCR assay was used to detected the expression of SNHG12 in control, NC, si-SNHG12-1, si-SNHG12-2 and si-SNHG12-3 group. (K) RT-PCR assay was used to detected the expression of hsa-miR-181a-5p and hsa-miR-138-5p in control, NC and si-SNHG12-3 group. (L and M) The dual luciferase reporting assay was used to verify the binding of SNHG12 to hsa-miR-181a-5p and hsa-miR-138-5p. Notes: *p<0.05, **p<0.01, ***p<0.001 compared with control.

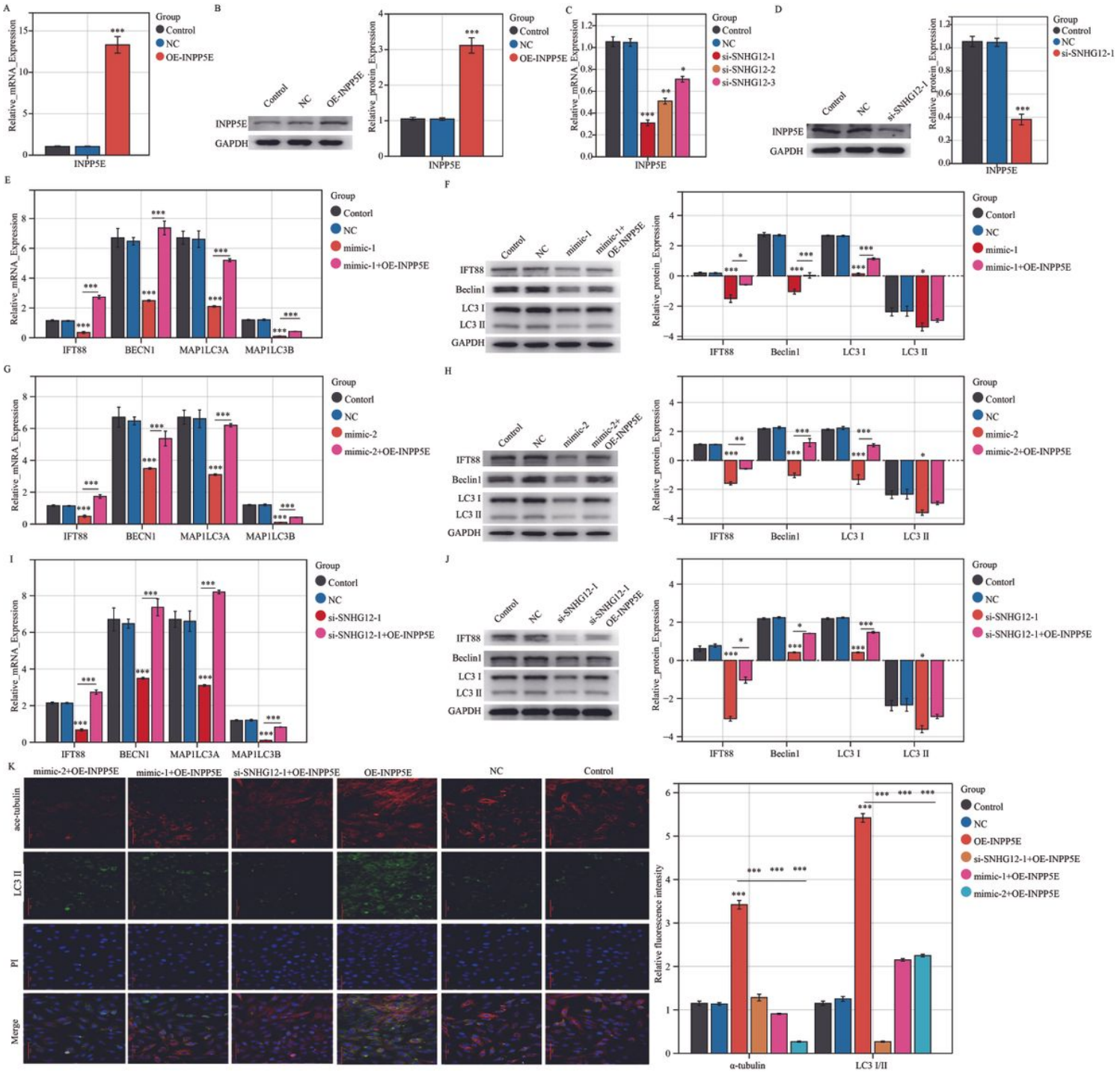

Figure 4

Silencing SNHG12 promotes primary cilia and autophagy via hsa-miR-181a-5p/hsa-miR-138-5p-INPP5E axis in vitro. (A and B) RT-PCR and WB assay were used to detected the expression of INPP5E in control, NC and OE-INPP5E group. (C and D) RT-PCR and WB assay were used to detected the expression of INPP5E in control, NC and si-SNHG12 group. (E and F) RT-PCR assay was used to detected the mRNA expression of IFT88, Beclin1, MAP1LC3A and MAP1LC3B, and WB assay was used to detected the protein expression of IFT88, Beclin1, LC3 I and LC3 II in control, NC, mimic-1 and mimic-1 + OE-INPP5E group. (G and H) RT-PCR assay was used to detected the mRNA expression of IFT88, Beclin1, MAP1LC3A and

MAP1LC3B, and WB assay was used to detected the protein expression of IFT88, Beclin1, LC3 I and LC3 II in control, NC, mimic-2 and mimic-2 + OE-INPP5E group. (I and J) RT-PCR assay was used to detected the mRNA expression of IFT88, Beclin1, MAP1LC3A and MAP1LC3B, and WB assay was used to detected the protein expression of IFT88, Beclin1, LC3 I and LC3 II in control, NC, si-SNHG12-1 and si-SNHG12-1 + OE-INPP5E group. (K) Ace-tubulin was used to labeled primary cilia and LC3 II was used to labeled autophagy via immunofluorescence assay. Notes: *p<0.05, **p<0.01, ***p<0.001 compared with control.

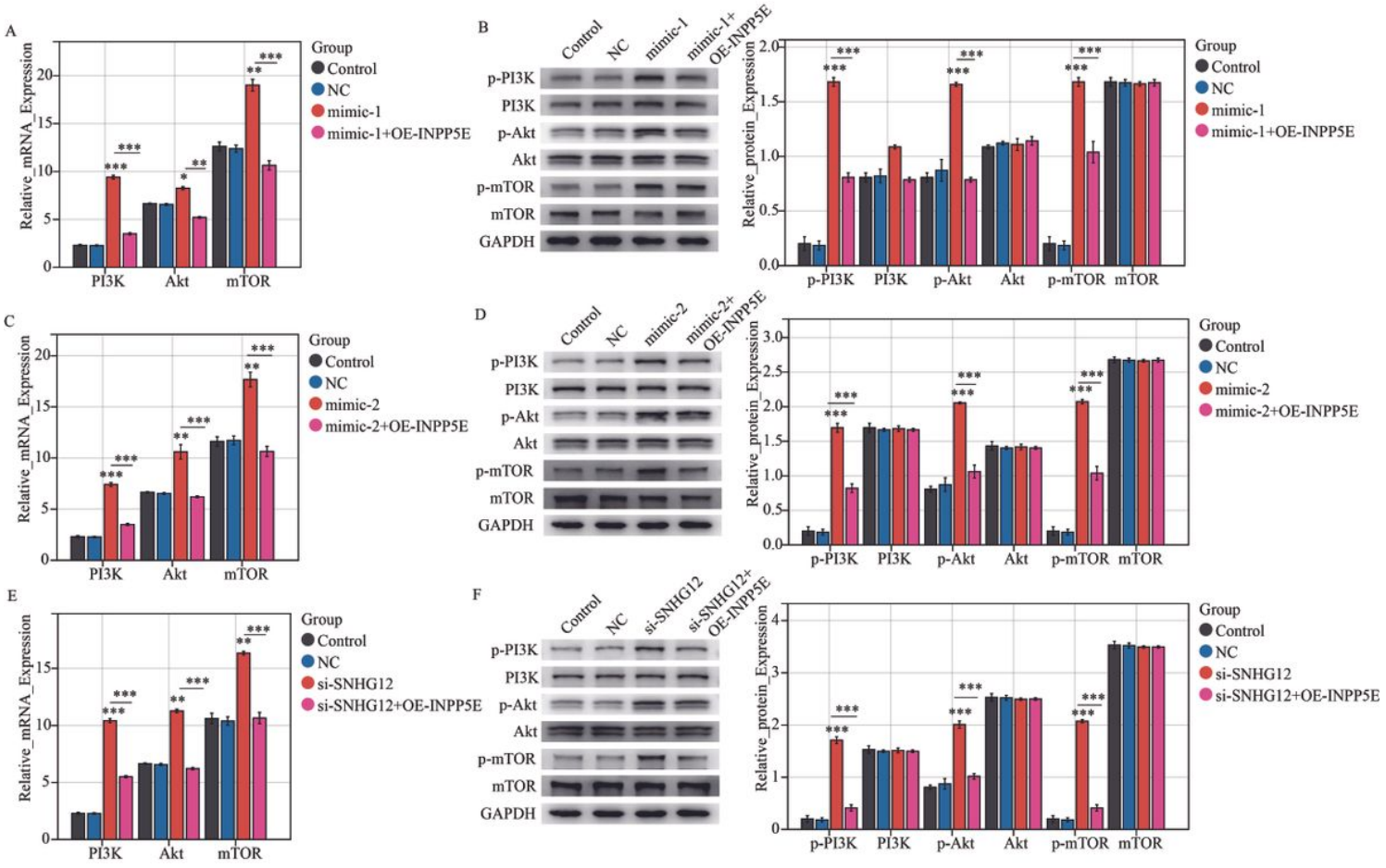

Figure 5

Silencing SNHG12 activated the PI3K-Akt-mTOR signaling pathway via hsa-miR-181a-5p/hsa-miR-138-5p-INPP5E axis in vitro. (A) RT-PCR assay was used to detected the expression of PI3K, Akt and mTOR in control, NC, mimic-1 and mimic-1 + OE-INPP5E group. (B) WB assay was used to detected the expression of PI3K, p-PI3K, Akt, p-Akt, mTOR and p-mTOR in control, NC, mimic-1 and mimic-1 + OE-INPP5E group. (C) RT-PCR assay was used to detected the expression of PI3K, Akt and mTOR in control, NC, mimic-2 and mimic-2 + OE-INPP5E group. (D) WB assay was used to detected the expression of PI3K, p-PI3K, Akt, p-Akt, mTOR and p-mTOR in control, NC, mimic-2 and mimic-2 + OE-INPP5E group. (E) RT-PCR assay was used to detected the expression of PI3K, Akt and mTOR in control, NC, si-SNHG12 and si-SNHG12 + OE-INPP5E group. (F) WB assay was used to detected the expression of PI3K, p-PI3K, Akt, p-Akt, mTOR and p-mTOR in control, NC, si-SNHG12 and si-SNHG12 + OE-INPP5E group. Notes: *p<0.05, **p<0.01, ***p<0.001 compared with control.

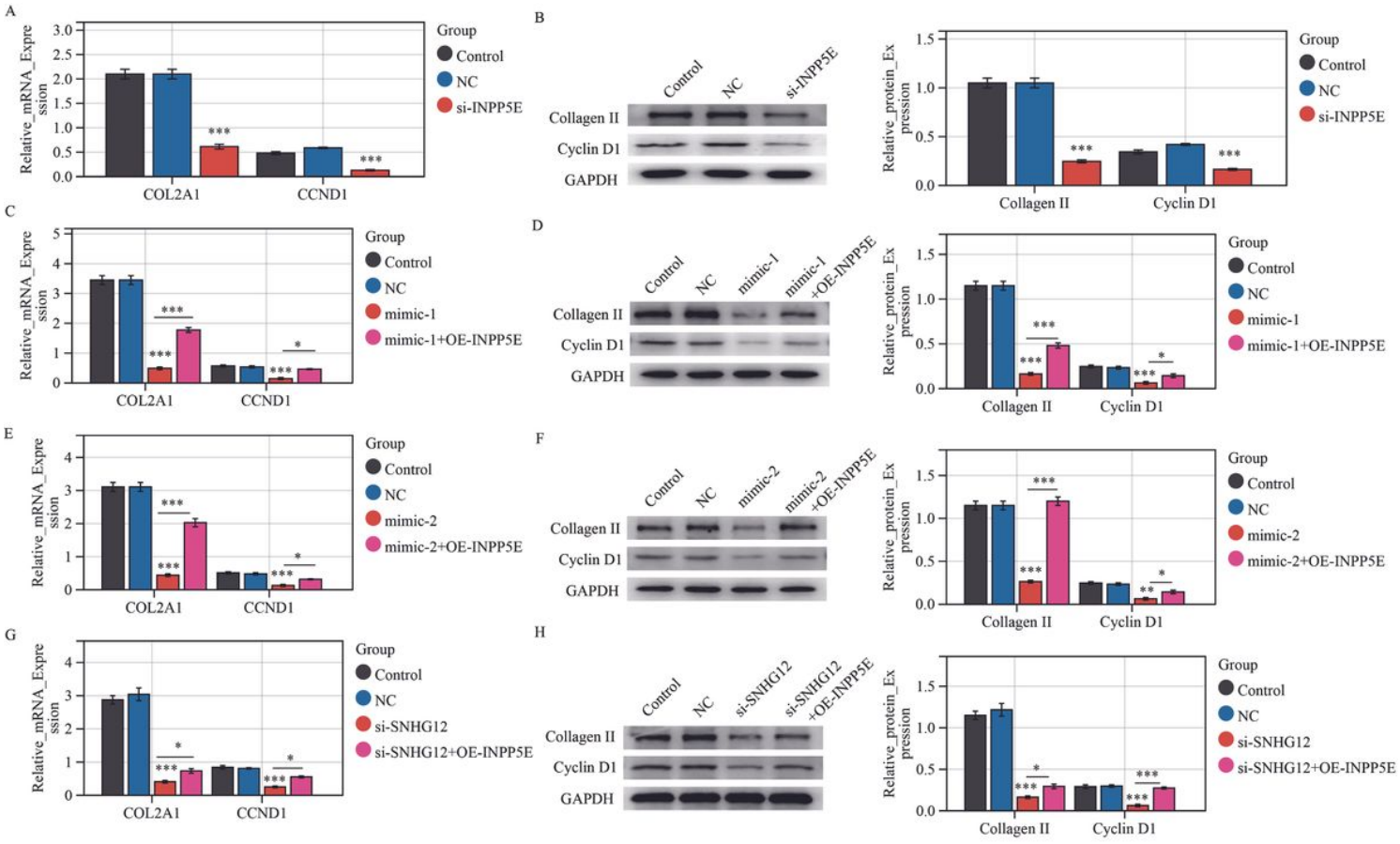

Figure 6

Silencing SNHG12 inhibits the expression of collagen II and cyclin D1 via hsa-miR-181a-5p/hsa-miR-138-5p-INPP5E axis in vitro. (A) RT-PCR assay was used to detected the expression of COL2A1 and CCND1 in control, NC and si-INPP5E group. (B) WB assay was used to detected the expression of collagen II and cyclin D1 in control, NC and si-INPP5E group. (C) RT-PCR assay was used to detected the expression of COL2A1 and CCND1 in control, NC, mimic-1 and mimic-1 + OE-INPP5E group. (D) WB assay was used to detected the expression of collagen II and cyclin D1 in control, NC, mimic-1 and mimic-1 + OE-INPP5E group. (F) RT-PCR assay was used to detected the expression of COL2A1 and CCND1 in control, NC, mimic-2 and mimic-2 + OE-INPP5E group. (F) WB assay was used to detected the expression of collagen II and cyclin D1 in control, NC, mimic-2 and mimic-2 + OE-INPP5E group. (G) RT-PCR assay was used to detected the expression of COL2A1 and CCND1 in control, NC, si-SNHG12 and si-SNHG12 + OE-INPP5E group. (H) WB assay was used to detected the expression of collagen II and cyclin D1 in control, NC, si-SNHG12 and si-SNHG12 + OE-INPP5E group.

Supplementary Files

This is a list of supplementary files associated with this preprint. Click to download.

- Supplementtables.docx

- SupplementFigure1.jpg